Published in the Russian Federation
European Geographical Studies
Has been issued since 2014.
ISSN: 2312-0029
Vol. 7, Is. 3, pp. 137-145, 2015

DOI: 10.13187/egs.2015.7.137
www.ejournal9.com

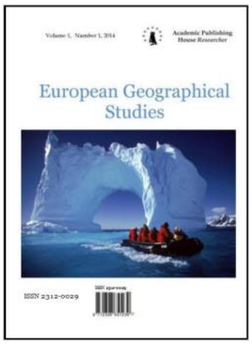


UDC 528.854.2

# Application of Remote Sensing Technique to Detect Copper Mineral based Principal Component Analysis and Band Ratio Methods. A Case Study: Laocai Province, Vietnam

[1] Le Hung Trinh
[2] Danh Tuyen Vu

[1] Le Quy Don Technical University
236 Hoang Quoc Viet Street, Hanoi, Vietnam
Candidate of Technical Sciences
E-mail: trinhlehung125@gmail.com
[2] Hanoi University of Natural Resources and Environment
Phu Dien, Hanoi, Vietnam
Candidate of Technical Sciences
E-mail: vdtuyen@hunre.edu.vn

**Abstract**

Remote sensing technology with advantages such as wide area coverage and short revisit interval has been used effectively in the study of mineral mining and exploration. This article presents study on application of principle component analysis and band ratio method to detect copper mineral using multispectral image LANDSAT 7 ETM+ in Laocai province, the Northern of Vietnam. The results which are obtained in this study can be used to create distribution copper map, and to serve mineral mining and exploration.

**Keywords**: remote sensing, copper, monitoring, principal component analysis, band ratio, Landsat

## 1. Introduction

Located in Southeast Asia, Vietnam is rich in mineral resources. Mineral resource is one of the most important natural resources of Vietnam. Mineral is the source material for many industries, such as energy production, building-materials, metal, agricultural and industrial sections... The exploration of mineral composite is a complex and urgent problem in researching and monitoring natural resource. Traditional methods based on field surveys only solve the problem on a small scale because of the high cost. Remote sensing technology with advantages such as wide area coverage and short revisit interval has been used effectively in the study of mineral mining and exploration.

To detect and monitor minerals, researches in various countries have used remote sensing data, mainly Landsat and Aster optical images with average spatial resolution (Abdelsalam et al., 2000; Ramadan et al, 2001; Madani et al., 2003; Ramadan, Kontny, 2004; Maruthi Sridhar, Vincent 2009; Fraser et al., 1997...) [1, 3-8]. In these studies, the authors have been used difference methods, such as band rationing method (Clay mineral index, Iron oxide index, Ferrous minerals index) [1, 6], principal component analysis method based Crosta technique [3], Least square fitting method (LST) and Minimum noise fraction method (MNF) [3, 8]. Moreover, three band ratio images can be combined as color composites which highlight certain features in distinctive colors (Abrams index, Chica – Olma index, Kaufmann index) [3]. In Vietnam also had some studies in application of remote sensing technique to detect and monitoring clay minerals, iron oxide [10-13].

In this paper, the authors analyze the spectral characteristics of copper mineral to detect copper mineral in Laocai province, the Northern of Vietnam using Landsat 7 ETM+ multispectral images.

## 2. Study area and Materials

**Study area**. The Laocai province is located in the Northern of Vietnam, about 338 km of Hanoi, the capital of Vietnam. The area is bounded by 22º22'48" N latitude and 104º09'28" E longitude (Figure 1). The province covers an area of 6383.9 km² and had a population of 656900 people [16].

The province has rich mineral resources, 30 types have been identified with good reserves. The major valuable mineral reserves are: copper (about 53 million tons), apatite and iron (2.5 million tons), molybdenum (15 million tons). There are 150 mines in the province exploiting various minerals [16].

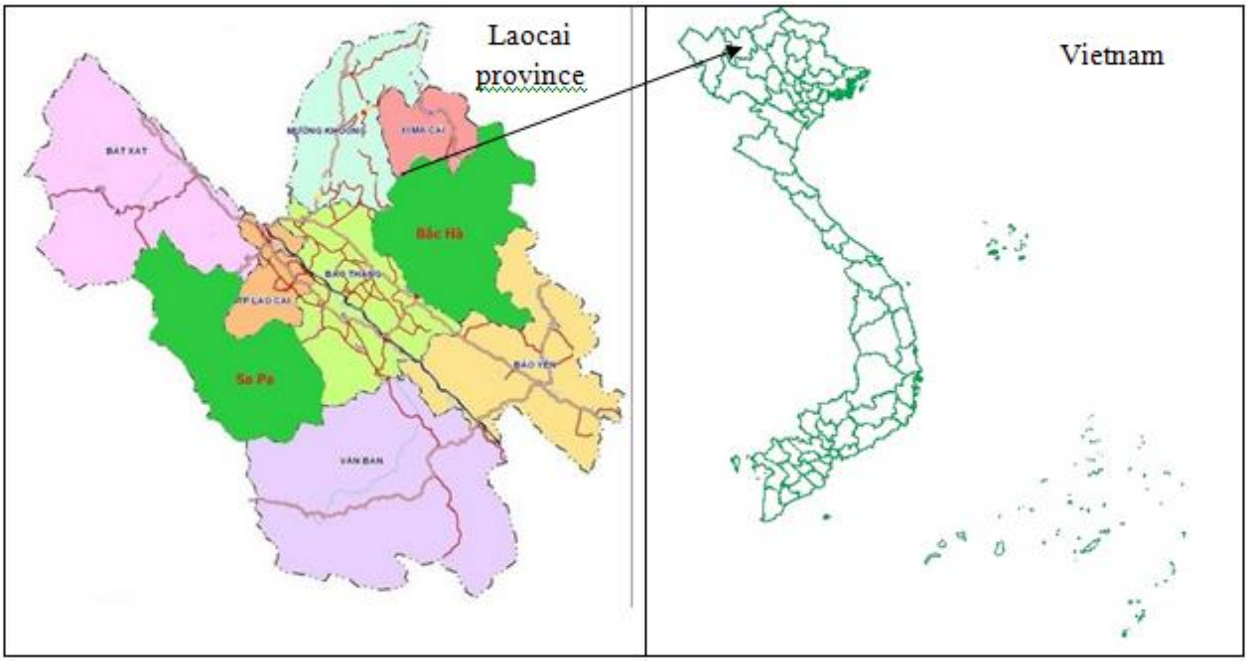


Figure 1. The study area, Laocai province (Vietnam)

**Data used**. In this study, multi-spectral cloud – free Landsat 7 Enhanced Thematic Mapper Plus (ETM+) data in 20 September 2007 was collected (Figure 1). The Landsat 7 ETM+ data was the standard terrain correction products (L1T), downloaded from United States Geological Survey (USGS – http://glovis.usgs.gov) website [17]. Landsat 7 ETM + images consist of eight spectral bands with a spatial resolution of 30 m for band 1 to 5 and 7. Spatial resolution for thermal infrared band (band 6) is 60 m, but is resampled to 30 m pixels. Band 8 (0.52 – 0.90 μm) is the panchromatic with spatial resolution of 15 m (Table 1) [14].

Table 1: LANDSAT 7 ETM+ characteristics

| No. | Band | Wavelength (μm) | Spatial resolution (m) |
|---|---|---|---|
| 1 | Blue | 0.45 – 0.515 | 30 |
| 2 | Green | 0.525 – 0.605 | 30 |
| 3 | Red | 0.63 – 0.69 | 30 |
| 4 | NIR | 0.75 – 0.90 | 30 |
| 5 | MIR | 1.55 – 1.75 | 30 |
| 6 | TIR | 10.40 – 12.50 | 60 |
| 7 | MIR | 2.09 – 2.35 | 30 |
| 8 | PAN | 0.52 – 0.90 | 15 |

Figure 2. Landsat 7 ETM+ multispectral image of the Laocai province 20 September 2007, 321/RGB color composite

### 3. Methodology

**Spectral characteristic of copper.** Figure 3 shows reflectance spectra of copper. The vertical axis shows the percentage of incident sunlight that is reflected by the materials [2]. The horizontal axis shows wavelengths of energy for the visible spectral region (0.4 to 0.7 μm) and the reflected portion (0.7 to 3.0 μm) of the infrared (IR) region. Reflected infrared energy consists largely of solar energy reflected from the earth at wavelengths longer than the sensitivity range of the eye.

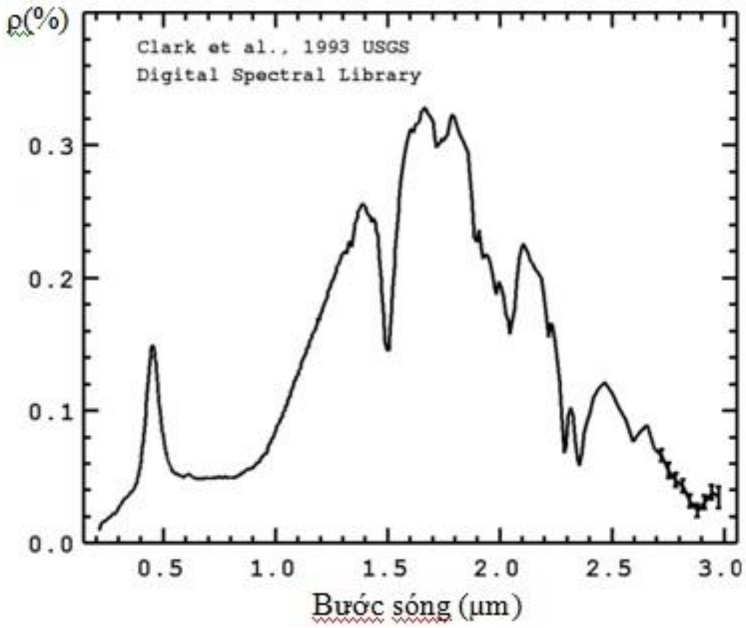


Figure 2. Spectral characteristic of copper minerals in visible and infrared wavelet

**Image pre-interpretation.** Image processing started with radiometric and geometric correction. Radiometric correction done by converted the digital number value to radiance value. Based on NASA model, the digital values of Landsat 7 ETM+ bands were converted to spectral radiance ($Wm^{-2}\mu m^{-1}$) using following equation [14]:

$$L_\lambda = \frac{Lmax_\lambda - Lmin_\lambda}{Q_{calmax} - Q_{calmin}}(Q_{cal} - Q_{calmin}) + Lmin \qquad (1)$$

Where

$L_\lambda$ - Spectral radiance at the sensor's aperture [$W/(m^2.sr.\mu m)$]
$Q_{cal}$ – Quantized calibrated pixel value
$Q_{calmax}$ – Maximum quantized calibrated pixel value corresponding to $Lmax_\lambda$
$Q_{calmin}$ – Minimum quantized calibrated pixel value corresponding to $Lmin_\lambda$
$Lmax_\lambda$ - Spectral at sensor radiance that is scaled to DNmax [$W/(m^2.sr.\mu m)$]
$Lmin_\lambda$- Spectral at-sensor radiance that is scaled to DNmin [$W/(m^2.sr.\mu m)$]

Table 2: LANDSAT ETM+spectral radiance $Q_{calmax}$, $Q_{calmin}$ dynamics ranges [14]

| No. | Band | Wavelength | $Q_{calmax}$ | $Q_{calmin}$ |
|---|---|---|---|---|
| 1 | Blue | 0.45 – 0.515 µm | 191.600 | -6.200 |
| 2 | Green | 0.525 – 0.605 µm | 196.500 | -6.400 |
| 3 | Red | 0.63 – 0.69 µm | 152.900 | -5.000 |
| 4 | NIR | 0.75 – 0.90 µm | 241.100 | -5.100 |
| 5 | MIR | 1.55 – 1.75 µm | 31.060 | -1.000 |
| 7 | MIR | 2.09 – 2.35 µm | 10.800 | -0.350 |

In the second step, for relatively clear Landsat scenes, reflectance (the TOA reflectance) can be determined from the spectral radiance data. The TOA reflectance is computed according to the equation:

$$\rho_\lambda = \frac{\pi.L_\lambda.d^2}{ESUN_\lambda.\cos(\theta_s)} \qquad (2)$$

Where
$\rho_\lambda$ – planetary TOA reflectance
$\pi$ – mathematical constant approximately equal to 3.14159
$L_\lambda$ – spectral radiance at the sensor's aperture

D – Earth – Sun distance (astronomical units), which calculate following equation:

$$d = (1{,}0 - 0{,}01674.\cos(0{,}9856(D-4))) \quad (3)$$

D – the day number of the year

ESUN – Mean exoatmospheric solar irradiance ($W/m^2.sr.\mu m$) (Table 2) [14];

θs – solar zenith angle (degree) [14].

Table 2: ESUN values for LANDSAT ETM+ images

| No. | Band | Wavelength | ESUN (watts/m².ster. µm) |
|---|---|---|---|
| 1 | Blue | 0.45 – 0.515 µm | 1997 |
| 2 | Green | 0.525 – 0.605 µm | 1812 |
| 3 | Red | 0.63 – 0.69 µm | 1533 |
| 4 | NIR | 0.75 – 0.90 µm | 1039 |
| 5 | MIR | 1.55 – 1.75 µm | 230.8 |
| 7 | MIR | 2.09 – 2.35 µm | 84.90 |
| 8 | PAN | 0.52 – 0.90 µm | 1362 |

The surface reflectance value can be calculated using atmospheric correction method DOS – "dark object subtraction". The DOS is a family of image based atmospheric correction method proposed by Chavez (1988). The basic assumption is that within the image, some pixels are in complete shadow and their radiances received at the satellite are due to mathospheric scattering (path radiance) [9].

**Band ratio.** Band ratio is a useful method of preprocessing satellite image, especially in areas where topographic effects are important. The band ratio images are known for enhancement of spectral contrast among the bands considered in the ratio operation and have successfully been used in mapping alteration zones [3-8]. As shows in the figure 2, the spectral reflectance curve shows that the maximum reflectance of copper occurs in blue (band 10.45 – 0.515 µm) and red band (band 3, 0.63 – 0.69 µm) and that reflectance is considerably lower in middle infrared bands (band 5, 1.55 – 1.75) and band 7 (2.09 – 2.35). There form, the brightness signatures in the ratio images band5/band1 and band7/band3 correlate with the copper mineral [3-7].

**Principal component analysis**. The principal component analysis (PCA) method is based on the fact that neighboring bands of multispectral images are highly correlated and often convey almost the same information about the object. This method is based on multivariate statistical technique that selects uncorrelated linear combination (eigenvector) of variables in such a way that each successively extracted linear combination – principal component [7]. This study has used principal component analysis method for ratio images band5/band1 and band7/band3 of Landsat 7 ETM+ data. Table 3 shows the results of calculation Eigen matrix and eigenvalues. The first principal component (PC1) is about 99.5% and the second principal component (PC2) is about 0.5% of eigenvalue of the total variance for unstretched data PCA. Thereform, PC1 is the albedo image and PC2 highlights cooper minerals as bright pixels.

Figure 3 shows the model for detecting and extracting copper minerals from Landsat 7 ETM+ multispectral images.

Table 3. Eigen matrix and Eigenvalues

| Band ratio / PC | Band5/Band1 | Band7/Band3 | Eigenvalues (%) |
|---|---|---|---|
| PC1 | 0.74301 | -0.66927 | 99,5% |
| PC2 | 0.66927 | 0.74301 | 0.5% |

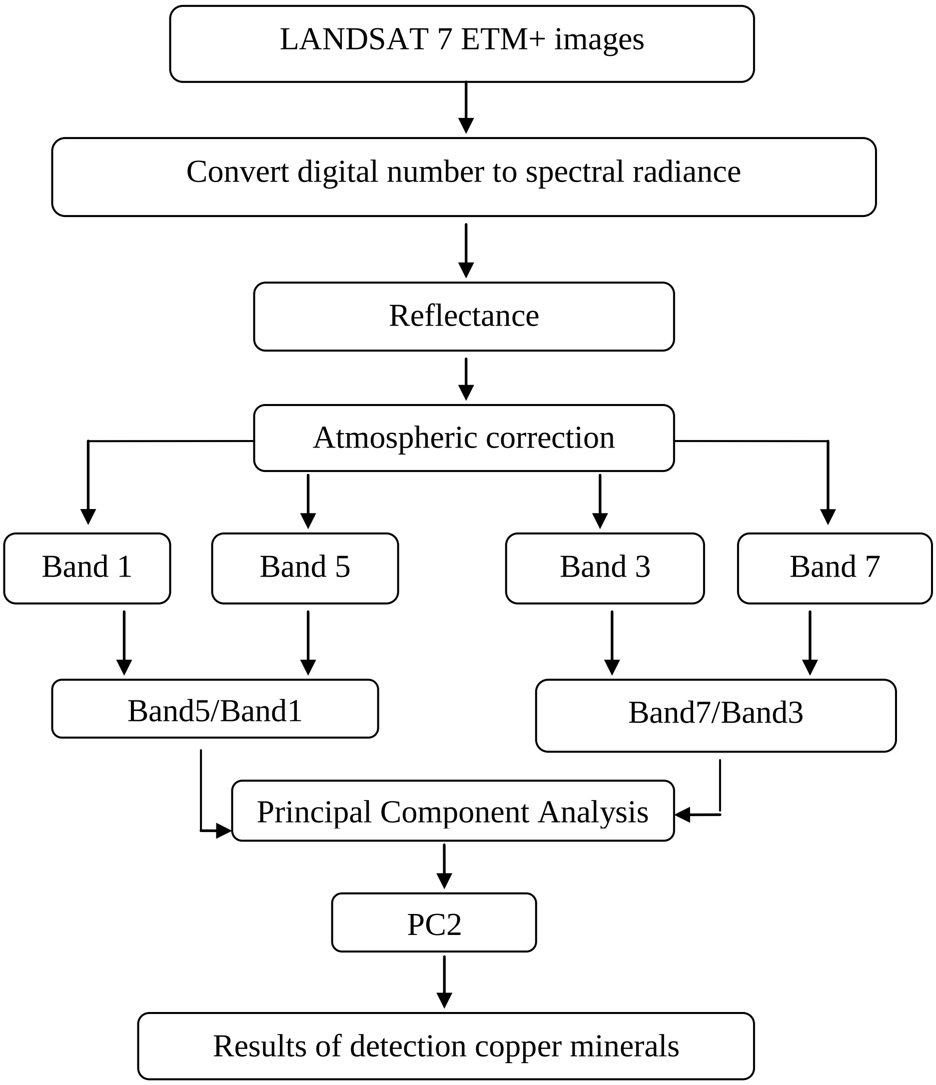


Figure 3. Model for detecting copper minerals using LANDSAT 7 ETM+ image

## 4. Results and Discussion

The Landsat 7 ETM+ data in this study have been used to calculate band5/band1 and band7/band3 ratio images (figure 4a, 4b). This ratio images enhanced copper minerals as bright pixel values.

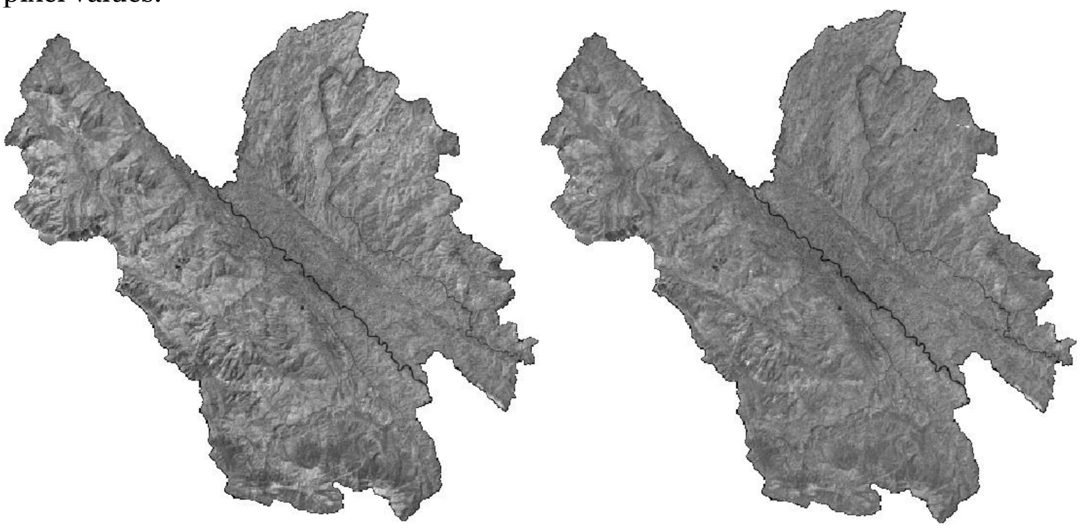

*a)* *b)*

Figure 4. Band ratio images band5/band1 (a) and band7/band3 (b) LANDSAT 7 ETM+

The principal components transformation on ratio images band5/band1 and band7/band3 of the Laocai province, the Northern of Vietnam are show in table 3 and figure 5 (a, b).

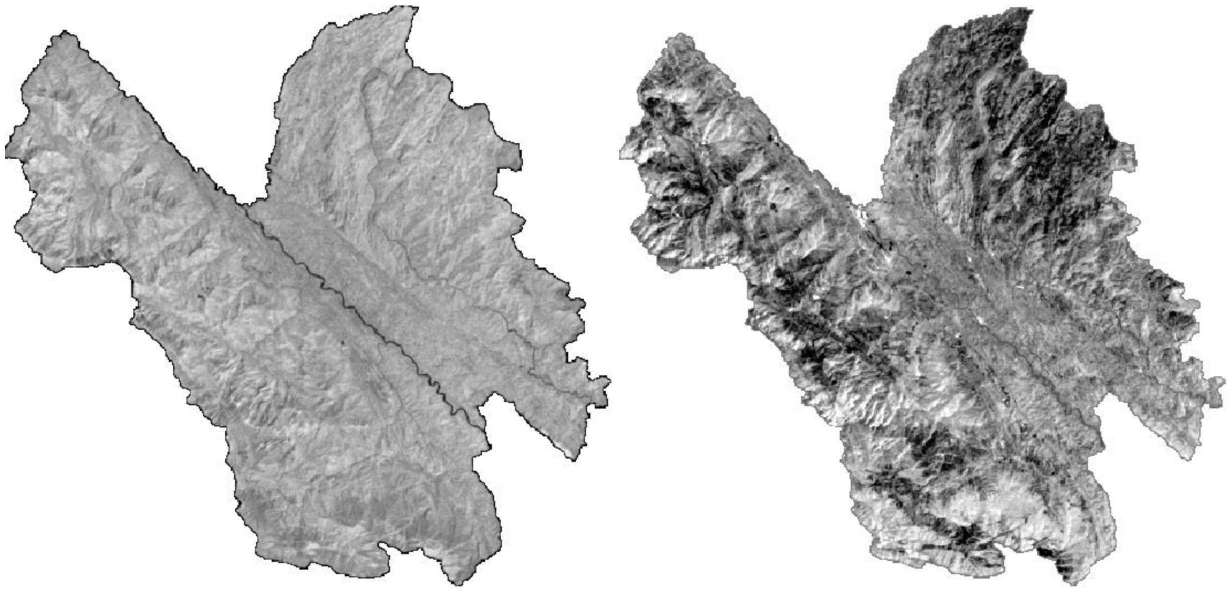

*PC1* *PC2*

Figure 5. The first (PC1) and second (PC2) principal components based on band ratio images

To evaluate accuracy, the mineral map at a scale of 1: 200 000 of Laocai province was used [15]. Analysis of results obtained from this study show that, the copper deposits detected from Landsat 7 ETM+ multispectral image consistently with mineral map, such as Suoi Thau, Sinh Quyen, Tong Cao Chay, Ban Vuoc, Lung Thang, Quang Kim, Ta Phoi...copper deposits (Figure 6). It also proves the accuracy of the principal component analysis method in detection copper mineral from remote sensing data.

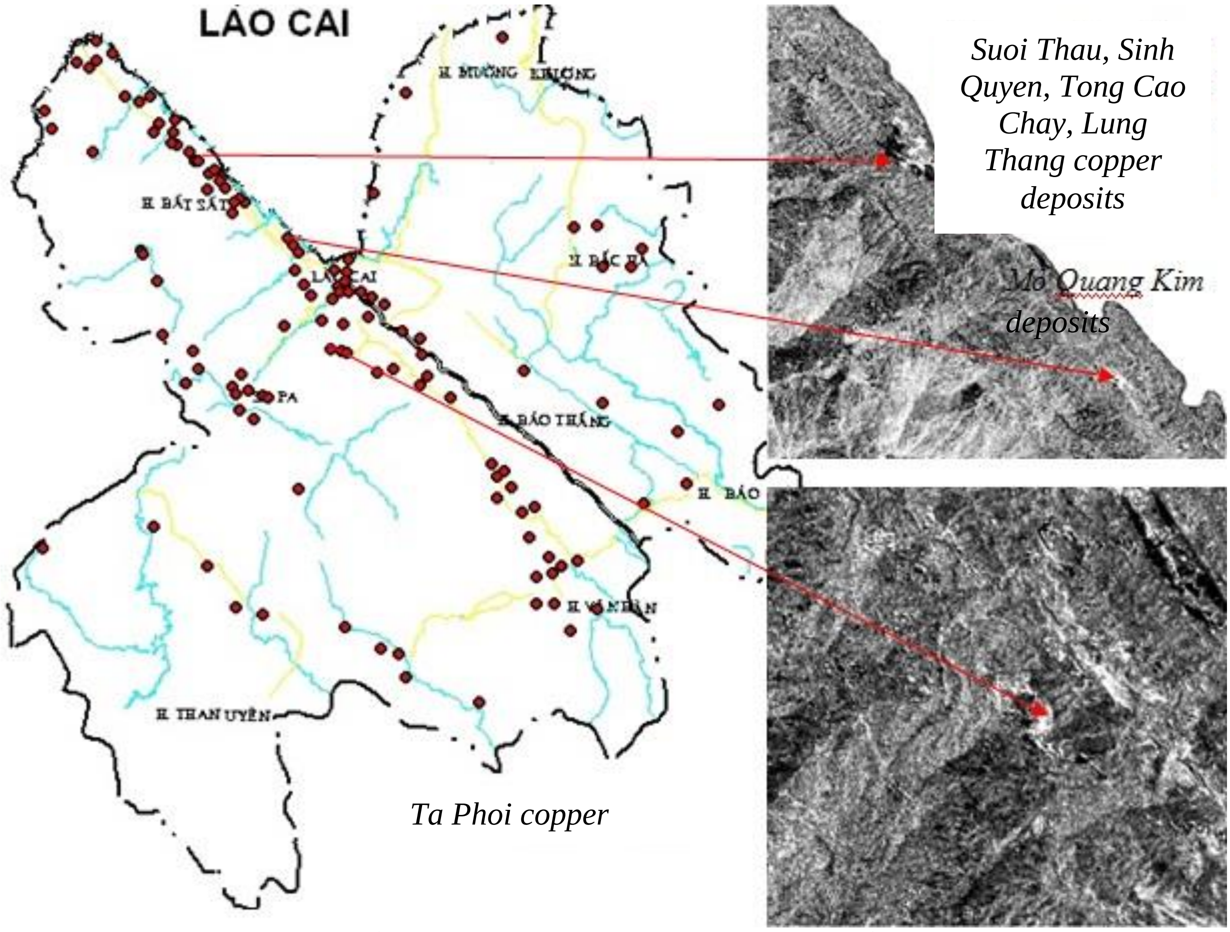


Figure 7. Mineral map of Laocai province, Vietnam at a scale of 1:200 000 and copper deposits in Landsat image

**5. Conclusion**

Remote sensing technique with many advantages, compared with traditional methods, can be used effectively for detecting and predicting the density distribution of mineral. Analysis of spectral characteristics of copper mineral shows that, the band 5/1 and 7/3 ratios are sensitive to the copper mineral, such that areas of high 5/1 and 7/3 values have relatively high copper contents.

Principal component analysis is widely used for mapping and detecting of mineral. This technique is used on 2 ratio images: band5/band1 and band7/band3 for enhancing copper mineral. The results which are obtained in this study can be used to create distribution copper mineral and to serve mineral mining and exploration.

**References:**

1. Maruthi Sridhar B.B., Robert K. Vincent (2009). *Mapping and estimation of phosphorus and copper concentrations in Fly Ash spill area using LANDSAT TM data*, Photogrammetric Engineering and remote sensing 75(9), 1030–1033.

2. Clark R.N., Swayze G.A., Wise R., Livo K.E., Hoefen T.M., Kokaly R.F., Sutley S.J. (1993). *USGS Digital Spectral library*, USGS Open file Rep.

3. Crosta A.P., Moore J.M. (1989). *Enhancement of LANDSAT Thematic Mapper imagery for residual soil mapping in SW Minas Gerais State Brazil: a prospecting case history in greenstone belt terrain*, Proceedings of the 9th Thematic Conference on Remote Sensing for Exploration Geology, Calgary (Ann Arbor, MI: Environmental Research Institute of Michigan), pp. 1173–1187.

4. Amro F. Alasta (2011). *Using remote sensing data to indentify iron deposits in central western Libya*, International conference on Emerging trends in Computer and Image processing, Bangkok, pp. 56 – 61.

5. Dematte J.A.M., Fiorio P.R., Ben-Dor E (2009). *Estimation of soil properties by orbital and laboratory reflectance means and its relation with soil classification*, The open Remote sensing journal, Vol. 2, pp.12 – 23.

6. Hankan Mete Dogan (2012). *Mineral composite assessment of Kelkit River Basin in Turkey by means of remote sensing*, Journal Earth System Science, 118(6), pp.701 - 710.

7. Md. Bodruddoza Mia, Yasuhiro Fujimitsu (2012). *Mapping hydrothermal altered mineral deposits using LANDSAT 7 ETM+ image in and around Kuju volcano, Kyushu, Japan*, Journal Earth System Science, 121(4), pp.1049 – 1057.

8. Fraster S.J., Green A.A. (1997). *A software defoliant for geological analysis of band ratio, International journal of remote sensing*, Vol.8, 525 – 532.

9. Chavez P.S. (1988). *An improved dark-object subtraction technique for atmospheric scattering correction of multispectral data*, Remote Sensing of Environment, Vol. 24. pp. 459–479

10. Trinh Le Hung (2013). *Application of band rationing method for detecting iron oxide, clay minerals and ferrous minerals*, Mining industry journal, Vol.4, pp. 19 – 24.

11. Trinh Le Hung (2014). *Application of remote sensing to detect iron composite and clay minerals based Crosta technique*, Mining industry journal, Vol. 1, pp. 36 – 40.

12. Trinh Le Hung (2013). *The method of analyzing the principal components to detect clay minerals and iron oxide distribution using images from LANDSAT satellite*, Journal of Science, Ho Chi Minh National university of education, Vol. 10, pp. 147 – 156.

13. Dao Khanh Hoai, Nguyen Sach Thanh, Nguyen Van Hung (2013). *Application of directed principal component analysis method to detect clay minerals*, Mining industry journal, Vol.2B, pp. 67 – 70.

14. LANDSAT Conversion to Radiance, Reflectance and At-Satellite Brightness Temperature (NASA).

15. Minerals map of Laocai province, 1:200 000, http://idm.gov.vn

16. *www.baolaocai.vn*

17. *USGS,* http://glovis.usgs.gov